Relaxation Dynamics and Transient Behavior of Small Arenethiol Passivated Gold Nanoparticles

Michael Busby,*,† Claudio Chiorboli,‡ and Franco Scandola*,†,‡

Dipartimento di Chimica, Università di Ferrara, and INSTM, Sezione di Ferrara, 44100 Ferrara, Italy, and ISOF-CNR, Sezione di Ferrara, 44100 Ferrara, Italy

Received: December 1, 2005; In Final Form: February 6, 2006

Novel gold nanoparticles, passivated by monolayers of benzenethiol, biphenylthiol, and similar derivatives, have been synthesized and characterized using UV/vis, NMR, and Fourier transform infrared (FTIR) spectroscopies. The nanoparticle sizes have been evaluated using transmission electron microscopy and UV/vis spectroscopy; they show diameters between 2.1 and 4.7 nm, depending on the method of synthesis and the monolayer protecting group. Femtosecond transient absorption measurements show that the nanoparticles possess optical properties on the boundary between molecular and nanoparticle behavior. The smaller systems based on benzenethiol exhibit long-lived excited states with lifetimes on the order of a few nanoseconds, resembling those of small gold molecular type clusters. The larger nanoparticles protected with biphenylthiol and benzylthiol groups relax much more rapidly on a picosecond time scale, similarly to related citrate stabilized systems reported in the literature.

Introduction

The first synthesis of novel organothiol−gold based monolayer protected clusters (MPCs) by Brust[1] 10 years ago has opened up new avenues into studying the optical properties of these hybrid systems. The presence of the covalently bound, passivating monolayer is known to alter the solubility, stability, and electronic properties of the nanoparticles, as well as allowing them to be functionalized with a wide variety of electrochemically, photophysically, and biologically active units.[2,3] Understanding the behavior of the nanoparticles' optical properties upon formation of the Au−S covalent bond is of great interest. Both experimental and theoretical studies[4] provide insight into how the surface plasmon and other cluster based absorptions can be altered by chemical means. A sound understanding of the nanoparticle based absorptions will also present a useful basis for comprehending the excited-state behavior of molecular chromophores tethered to metal cores.[5] This type of knowledge may be crucial to the design of molecular photonic materials and devices.[6−9]

The vast majority of work published on monolayer protected nanoparticles has been based on saturated alkanethiol systems.[3,10,11] Until recently,[12] sporadic interest has only been given in the literature to the aromatic, *arene*thiol based analogues. Synthesis of *p*-mercaptophenol nanoparticles was first published by Brust[13] in 1995. Since then, the synthesis of benzenethiol and other arenethiol nanoparticles has been afforded with two-phase synthesis.[12,14] These systems have been studied for their quantum capacitance properties and show behavior similar to that of their alkanethiol counterparts. Benzenethiol and derivatized benzenthiol nanoparticles have also been synthesized using the one-phase method,[15,16] to investigate their properties in films for chemical vapor sensing applications. Recently, thiol derivatized terpyridine nanoparticles have been synthesized and have been shown to form stable complexes with zinc.[17] Addition of thiophenol and benzyl mercaptan to anion stabilized gold nanoparticles induces aggregation, a process that results in a red shift and broadening of the surface plasmon resonance.[18]

The absorption spectrum of nanoparticles is a result of interband electronic transitions as well as surface plasmon resonance. Coherently oscillating conduction electrons, localized on the particle surface, couple to the electromagnetic field of light,[19] giving rise to surface plasmon absorption. UV/vis spectral measurements of the benzenethiol systems previously reported are based on nanoparticles with an average core diameter of 6.5 nm, and all show distinct surface plasmon bands between 575 and 522 nm, depending on the reactant ratios.[14] Theoretical and experimental studies on chromatographically separated, narrow size distribution alkanethiol stabilized nanoparticles between 1.4 and 3.2 nm[10] have shown the intensity of the surface plasmon to grow, with increasing size, resulting in a defined surface plasmon band at 2.4 eV (517 nm) for the 3.2 nm particles. The intensity variation of the surface plasmon band as a function of wavelength $\sigma(\omega)$ can be explained through the dipole-only approximation of Mie theory.[10,20,21]

$$\sigma(\omega) = 9\epsilon_m^{3/2} V_0 \frac{\omega}{c} \frac{\epsilon_2(\omega)}{[\epsilon_1(\omega) + 2\epsilon_m]^2 + \epsilon_2^2(\omega)}$$

In the above expression ω is the frequency of the absorbing light, V_0 is the volume of the absorbing particle, ϵ_m is the is the dielectric constant of the embedding medium, and ϵ_1 and ϵ_2 are the real and imaginary dielectric constants of the absorbing solid. To obtain the size dependence of the surface plasmon, the dielectric constants ϵ_1 and ϵ_2 are decomposed into contributions from the Drude free electrons in the conduction band and 5d electrons which are responsible for interband transitions. These parameters are seen to be directly related to the ratio of scattering rates between the surface and bulk of the material. As the particle size decreases from ca. 3 nm, surface scattering becomes dominant and the surface plasmon resonance is seen to broaden

* Corresponding author. E-mail: snf@unife.it.
† Università di Ferrara and INSTM.
‡ ISOF-CNR.

10.1021/jp056995v CCC: $33.50
Published on Web 03/03/2006

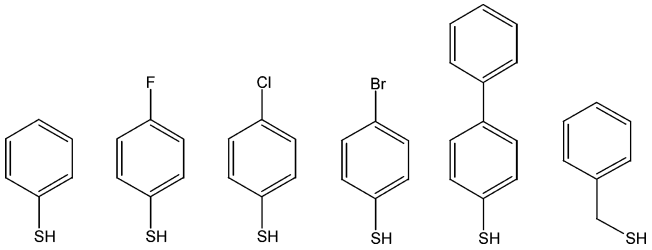

Figure 1. Arenethiol compounds used as passivating agents herein.

and red shift.[10,22] Furthermore, ϵ_m, the dielectric constant of the surrounding medium, can be modified by changing either the nanoparticle's passivating layer or the solvent in which it is dispersed.[4]

Below ca. 2−3 nm, nanoparticles exhibit "quantum size effects", where discrete electronic states are present and molecular traits are evident. In such circumstances the surface plasmon is also strongly dampened, and 5d−6sp type electronic transitions dominate the visible absorption spectrum.[10,20,21]

Ultrafast optical excitation of citrate stabilized gold[19] and alkanethiol passivated nanoparticles[23] with distinct surface plasmon bands (size greater than ca. 3 nm) show the broadening of the plasmon induced by a rapid formation of non-Fermi hot electron distribution. Spectrally, transient "wings" are seen in the visible, flanking the surface plasmon bleach. Kinetically, the excited electrons undergo ultrafast 100 fs electron/electron (e^-/e^-) relaxation, followed by electron/phonon (e^-/ph) relaxation between ca. 0.5 and 3 ps, and finally phonon/phonon (ph/ph) relaxation of generally hundreds of picoseconds.[19,23] The e^-/ph coupling mechanism in nanoparticles is similar to that observed in bulk metal.[24] The kinetics are seen to be laser power and surrounding medium dependent,[25] while independent of the nanoparticle size.[19,22,26] Experiments on anion stabilized gold nanoparticles show ph/ph coupling to be independent of laser power, whereas the surface area to volume ratio plays a significant role in the rate of energy dissipation from the excited nanoparticle to the solvent matrix. Kinetic lifetimes vary from 10 to 380 ps going from 5 to 50 nm diameter nanoparticles.[27]

Picosecond transient absorption spectra of 1.9 nm nanoparticles passivated with a dodecanethiol monolayer show a broad transient band with a maximum at ca. 480 nm, although a detailed kinetic analysis has not been performed.[23] Even smaller, 28-atom gold clusters exhibit a single band in the visible with decay dynamics well into the nanosecond time domain.[20]

In summary, the majority of absorption and femtosecond transient absorption spectra present in the literature are based on nanoparticle systems in the size regime above ca. 3 nm, while fewer examples exist of smaller systems where both the surface plasmon is dampened and the transition from bulk to molecular behavior occurs. Investigations into the optical properties of nanoparticles passivated by chemisorbed monolayers have been undertaken solely using saturated alkanethiol molecules. In principle, the physical properties of the monolayer will vary the dielectric constant of the nanoparticles surrounding medium[4,22] as well as modify the particle surface electron density,[10] thus affecting the optical properties of the nanoparticle itself.

In this article, the synthesis, characterization, and ultrafast spectroscopic behavior of benzenthiol nanoparticles and its bromo, chloro, and fluoro derivatives are presented; see Figure 1. Investigations are performed to ascertain whether systematic variations in the chemical properties of the monolayer (dielectric function and electron donation) will affect the shape and position of the electronic absorption spectrum, as well as the transient dynamics. Studies will also be performed on the novel biphenylthiol systems (see Figure 1), providing new insight into this previously unstudied area of nanoparticles.

Experimental Section

Chemicals. Bromobenzene, 4-(methylthio)phenylboronic acid, meta-chloroperbenzoic acid (mCPBA), hydrogen tetrachloroaurate trihydrate, benzenethiol, benzylthiol, 4-bromobenzenethiol, and 4-chlorobenzenethiol, were all obtained from Aldrich; 4-fluorobenzenethiol was obtained from Alfa Aesar. All nanoparticle synthesis were performed in glassware previously cleaned with aqua regia.

4-Methylsulfanylbiphenyl. A mixture of the 4-(methylthio)-phenylboronic acid (0.81 g, 4.81 mmol), ethanol (10 mL), bromobenzene (0.33 mL, 3.2 mmol), toluene (20 mL), and 2 M $Na_2CO_{3,aq}$ (10.6 mL) was degassed under Ar. Tetrakis-(triphenylphosphine) Pd(0) (155 mg, 0.13 mmol) was added, and the mixture was heated to reflux for 2 h. The mixture was warmed to room temperature, water was added (10 mL), and the compound was extracted in ethyl acetate 20 mL); the organic layers were combined, dried with anhydrous Na_2SO_4, and concentrated in vacuo. Purification on silica gel (cyclohexane/ethyl acetate 8:1) yielded 0.66 g (69%) of a white solid. ^{1}H NMR (δ/ppm, $CDCl_3$) 2.58 (s, 3H), 7.32−7.40 (m, 3H), 7.42−7.5 (m, 2H), 7.54−7.64 (m, 4H). ^{13}C NMR (δ/ppm, $CDCl_3$) 15.89, 126.81, 126.92, 127.18, 127.46, 128.78, 137.55, 138.02, 140.51.

Biphenyl-4-thiol-*S*-acetate. To a cooled (0 °C) and well-stirred solution of 4-methylsulfanylbiphenyl (0.48 g, 2.4 mmol) in dichloromethane (10 mL) was added mCPBA (0.604 g, 3.5 mmol). After 30 min $Ca(OH)_2$ (0.3 g, 4.05 mmol) was added, and the precipitate was filtered. Trifluoroacetic acid anhydride (0.695 mL, 5 mmol) was added to the filtrate, and the solution was heated to reflux for 2 h. The solvent was removed in vacuo, and the residue was dissolved in 20 mL of 50% methanol/TEA mixture. The solvent was evaporated in vacuo, dichloromethane (5 mL) and acetic anhydride (0.49 g, 4.8 mmol) were added, and the solution was stirred overnight at room temperature. The solvent was removed and the compound was purified over silica gel (cyclohexane/ethyl acetate 20:1), yielding a white solid (75% yield). ^{1}H NMR (δ/ppm, $CDCl_3$) 2.44 (s, 3 H), 7.4−7.6 (m, 5 H), 7.6−7.7 (m, 4 H).

Instrumentation. All spectroscopic measurements were performed using spectroscopic grade solvents. UV/vis spectra were measured using a Perkin-Elmer Lambda 40 spectrometer. Fourier transform infrared (FTIR) spectra were measured using a Bruker IFS 88 with the sample dispersed in a KBr pellet. NMR spectra were measured on a Varian Gemini spectrometer working at 300 MHz; the nanoparticles were dissolved in methylene chloride-d_2. Femtosecond transient spectroscopy was measured using a setup previously reported.[28] Transient kinetics were obtained using the exponential fitting algorithm of the Dynamic Surface Pro. software from Ultrafast Systems LLC. In time-resolved spectra, the first spectrun is taken immediately after chirp has subsided. Nanosecond flash photolysis measurements were performed using a setup as previously reported.[29] Transmission electron microscopic (TEM) samples were prepared by evaporating a drop of nanoparticles dissolved in dichloromethane (DCM) onto Formvar coated copper grids (Agar Scientific). They were subsequently left for 30 min for all traces of solvent to evaporate. Samples were imaged using a Hitachi H800 electron microscope (Japan) operating at 200 keV.

Results

Synthesis and Characterization of Nanoparticles. *Nanoparticle One-Phase Synthesis.* Nanoparticles passivated with

TABLE 1: Nanoparticle Average Sizes and Aromatic NMR Signal Positions of Arenethiol Nanoparticles Studied in This Work

nanoparticle	Ph-S-NP	Cl-Ph-S-NP	Br-Ph-S-NP	F-Ph-S-NP	biphenyl-S-NP	benzyl-S-NP
TEM size (std dev)/nm	2.1 (0.7)	2.1 (0.7)	2.3 (0.6)	2.3 (0.7)	3.2 (0.3)	4.7 (0.7)
NMR peak/ppm	7.05	7.15	7.05	7.00	7.05	

benzenethiol[15] and halogenated benzenethiols were synthesized based on Brust's procedure.[1] $HAuCl_3 \cdot 3H_2O$ (300 mg, 0.76 mmol) and the arenethiolate (1.8 mmol) were added to a solution of methanol (150 mL) and glacial acetic acid (3 mL). The gold was reduced upon addition of 22.3 mL of a 0.4 M aqueous solution of $NaBH_4$, added over a period of 1 min to the vigorously stirring solution. The solution was left stirring for a further 3 h. Then 50 mL of H_2O and 50 mL of DCM were added, and the organic phase was separated and dried over anhydrous sodium sulfate. The drying agent and any insoluble materials were then removed by filtration and the solution was reduced to a solid, in vacuo. The dark brown residue was resuspended in methanol with the aid of sonication and stirred for 2 h. The suspension was filtered over Celite and subsequently washed with 400 mL of methanol and 400 mL of acetonitrile to remove any excess arenethiolate and byproducts. The solid was washed of the Celite with DCM, the solvent was removed in vacuo, and the pure product was dried in a desiccator overnight.

Nanoparticle Two-Phase Synthesis. Nanoparticles passivated with biphenylthiol and benzylthiol were synthesized based on Brust's two-phase procedure.[1] $HAuCl_3 \cdot 3H_2O$ (350 mg, 0.88 mmol) was dissolved in 30 mL of H_2O and added to a solution of either biphenyl-4-thiol-*S*-acetate (267 mg, 1.17 mmol) or benzylthiol (145 mg, 1.17 mmol) in 80 mL of DCM. The aqueous phase was transferred into DCM upon addition of 1.6 g of tetraoctylammonium bromide (TOAB), and the mixture was subjected to vigorous stirring. The gold was reduced upon addition of 22.3 mL of a 0.4 M aqueous solution of $NaBH_4$, added over a period of 1 min to the vigorously stirring solution. The solution was left stirring for a further 3 h. Then 50 mL of H_2O and 50 mL of DCM were added, and the organic phase was separated and dried over anhydrous sodium sulfate. The drying agent and any insoluble materials were removed by filtration and the solution was reduced to a solid, in vacuo. The dark brown residue was resuspended in methanol with the aid of sonication and stirred for 2 h. The suspension was filtered over Celite and subsequently washed with 400 mL of methanol and 400 mL of acetonitrile to remove any excess arenethiolate, TOAB, and byproducts. The solid was washed of the Celite with DCM, the solvent was removed in vacuo, and the pure product was dried in a desiccator overnight.

NMR Spectra. NMR spectra of the benzenethiol passivated nanoparticles and derivatives all show broad featureless signals indicating the arenethiol is bonded to the surface.[30] The spectra showed no evidence of an equilibration between the arenethiol bonded to the surface and the arenethiol free in solution, an effect that would be seen immediately by the presence of sharp signals in the aromatic region, thus indicating the product is kinetically stable as well as free of residual synthetic components, within the sensitivity of the NMR spectrometer. Proton resonances are seen around 7 ppm for all the nanoparticles; see Table 1 (and Supporting Information for spectra).

UV/Vis Spectra. The UV/vis spectra of the benzenethiol nanoparticles and their halogenated derivatives were all measured in DCM, and all show very similar absorption spectra. No distinct surface plasmon maxima are seen to be present for any of the samples; in contrast, a broad featureless band is seen to cover the visible from 750 nm, forming a shoulder at 340 nm. At lower wavelengths for all the systems (<340 nm) an intense band is seen to absorb, resulting from $\pi \rightarrow \pi^*$ based transitions originating from the phenyl moiety of the passivating monolayer; see Figure 2.

The surface plasmon absorption of the biphenylthiol nanoparticles show a broad maximum in the visible at 500 nm. Further in the UV there is an absorption with a maximum at 276 nm; this band is also present in the absorption spectra of the free thiol at 273 nm and is thought to originate from $\pi \rightarrow \pi^*$ based transitions on the biphenyl moiety. Similarly, the benzylthiol nanoparticles exhibit absorptions in the visible with a broad maximum at ca. 490 nm. Absorptions in the UV are assigned to the benzylthiol moiety.

TEM. Average metal core sizes of the nanoparticles (Table 1) have been determined by TEM (Figure 3). The benzenethiol and 4-chlorobenzenethiol functionalized nanoparticles (Ph-NP and Cl-Ph-NP) have an average core size of 2.1 ± 0.7 nm, whereas 4-fluorobenzenethiol and 4-bromobenzenethiol functionalized nanoparticles (F-Ph-NP and Br-Ph-NP) are seen to be slightly larger by 0.2 nm, at 2.3 ± 0.6 and 2.3 ± 0.7 nm, respectively. The biphenylthiol- and benzylthiol-containing systems are seen to be definitely larger, at 3.2 ± 0.3 and 4.7 ± 0.7 nm, respectively. Size distribution histograms can be found in the Supporting Information. On the basis of the small standard

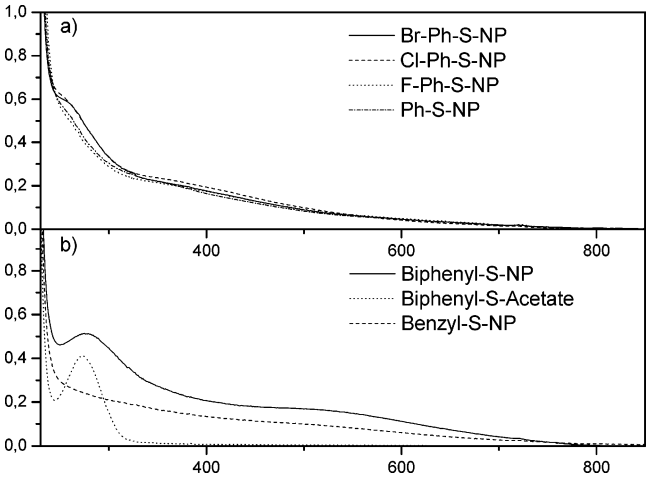

Figure 2. UV/vis absorption spectra: (a) benzenethiol type nanoparticles measured in dichloromethane and (b) biphenyl/benzylthiol type nanoparticles measured in dichloromethane.

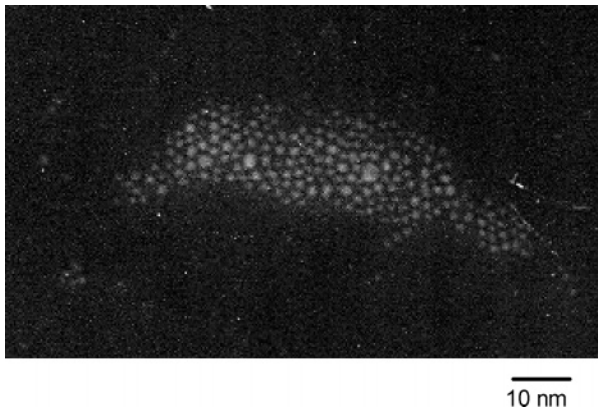

Figure 3. TEM image of benzenethiol gold nanoparticles.

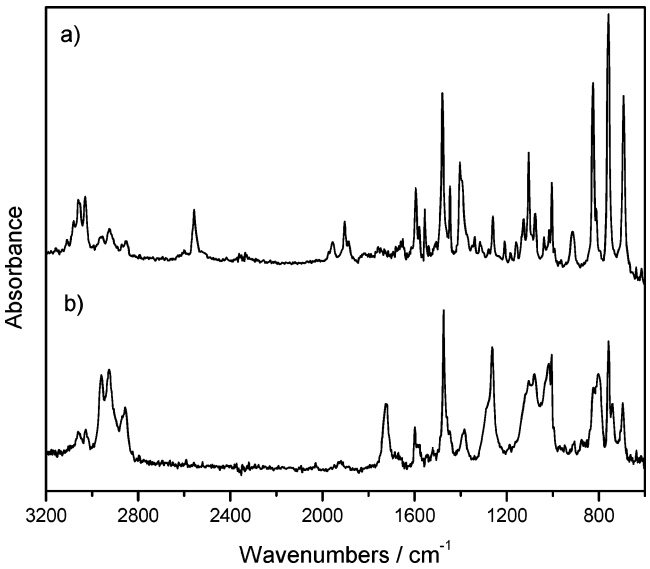

Figure 4. FTIR spectra of (a) biphenyl-4-thiol-*S*-acetate and (b) biphenylthiol nanoparticles measured in a KBr pellet.

deviations and the size distribution histograms, it can be concluded that the mean sizes are dominant in all cases.

FTIR Spectra. FTIR spectra of the biphenylthiol nanoparticles were measured dispersed in a potassium bromide pellet. Bands between 1400 and 1600 cm^{-1} are assigned to C═C stretching vibrations. Bands at higher energies between 3000 and 3100 cm^{-1} are assigned to aromatic C═C—H stretching vibrations. Similar vibrations are seen in the spectrum of the free biphenyl-4-thiol-*S*-acetate molecule. The similarity between the IR band signatures of the free molecule and those of the nanoparticles indicates their formation does not dramatically affect the chemical environment of the biphenyl moiety, as seen with other nanoparticle systems;[14] see Figure 4.

Transient Spectroscopy of Nanoparticles. Energy relaxation processes and dynamics of gold nanoparticles have been measured using femtosecond transient absorption spectroscopy. Excitation of the nanoparticles was performed at 400 nm in benzene with a 130 fs pulse fwhm (full width at half-maximum) of 0.005 mJ $pulse^{-1}$. Transient absorption spectra were subsequently probed in the visible range from 400 to 750 nm with a white light continuum.

The benzenthiol based nanoparticles show a transient signal formed within the instrumental response of 500 fs; see Figure 5. The broad signal is seen to cover the visible region, exhibiting a maximum at ca. 513 nm. The tail of a second band is seen growing toward the red starting at 700 nm, although the maximum is not seen due to the lack of white light beyond 750 nm. The signal is subsequently seen to decay between 0 and 3 ps by ca. 30%, although its structure is retained. Laser power dependence of the transient signal has been measured between 0.0012 and 0.01 mJ $pulse^{-1}$. Once the transient intensities have been normalized, it can be seen that decay rates are essentially identical within the error of the experiment. Between 3 ps and 1 ns, there is little change observed in the intensity and structure of the transient signal, indicating that its lifetime extends into the nanosecond domain. The initial component of the femtosecond data can be fitted to an exponential decay of ca. 1 ps. The lifetime of the long-lived component of the transient is ca. 15 ns, as measured in nanosecond flash photolysis (355 nm pump, deoxygenated benzene); see Figure 6. Similar transient structures and decay kinetics were observed for the 4-bromo-, 4-chloro-, and 4-fluorobenzenethiol systems.

The biphenylthiol nanoparticles were measured in benzene, under similar conditions. Transient signals are again present, immediately after excitation (Figure 7). In correspondence to the broad surface plasmon resonance absorption seen in the absorption spectrum, a transient bleach is observed with maximum amplitude at 555 nm. Flanking the bleach are two "wings" that increase in intensity from either side at 500 and 600 nm into the blue and red, respectively. The transient signal has reached its maximum directly after excitation, and subsequently undergoes decay between 0 and 5 ps, resulting in a flat baseline, indicating that the nanoparticles have returned to their equilibrated ground state. The decay is monoexponential with a lifetime of ca. 2 ps. Power dependence measurements were performed between 0.0016 and 0.0072 mJ $pulse^{-1}$. At all power intensities the transient signal was seen to have fully decayed by ca. 10 ps. No longer decay components were seen at any of the excitation powers.

Crude subtraction of the biphenylthiol spectra from that of the free passivating molecule in the UV indicates that, at 266 nm, 14% of the total absorption results from the biphenyl moiety. Due to absorption of benzene at this wavelength, transient absorption spectra were performed in tetrahydrofuran (THF) (which has a satisfactory transmission). The presence of a solvent transient covering most of the spectral region prevents any meaningful spectra from being recorded, although a transient absorption pertaining to the nanoparticles is seen between 700 and 750 nm. Decay kinetics of the this absorption can be fitted to a monoexponential lifetime of ca. 2.7 ps (Table 2). For comparison, transient spectra of biphenyl-4-thiol-*S*-acetate were also measured under the same conditions and showed that the molecular excited state has a lifetime into the nanosecond regime.

For the benzylthiol systems, a transient bleach is again seen at 555 nm; transient bands are present at either side of the bleach and reach into the red and blue. The signal decays from its maximum intensity directly after excitation to a flat baseline with a lifetime of ca. 4 ps; see Figure 8.

Discussion

Synthesis. Synthesis of benzenethiol nanoparticles and halogenated derivatives using the one-phase literature procedure with modified purification has worked successfully and produced pure samples of nanoparticles, as seen by the NMR spectra. Attempts to synthesize larger benzenethiol nanoparticles using the two-phase method were also made with a gold-to-thiol ratio of 1.1:1, but a stabilized nanoparticle system could not be obtained. Aggregation of some benzenethiol nanoparticles prepared using the two-phase method has previously been reported in the literature.[14]

Due to the incompatibility between solubility properties of the aqueous gold ions and the hydrophobic biphenylthiol, novel biphenylthiol protected nanoparticles have been synthesized using the two-phase method.[1] This method, in comparison to the one-phase synthesis, uses a smaller excess of arenethiol and yields a larger average size, as seen by UV/vis spectroscopy and the TEM measurements.

Benzenethiol Nanoparticles and Their Halogenated Derivatives. UV/vis spectra of benzenethiol nanoparticles synthesized by Brust's two-phase method have been reported previously.[14] These systems had average core diameters of 6.5 nm, and all showed distinct surface plasmon bands between 575 and 522 nm, depending on the reactant ratios and synthetic conditions, although aggregates were observed. The benzenethiol and halogenated benzenethiol nanoparticles reported herein have

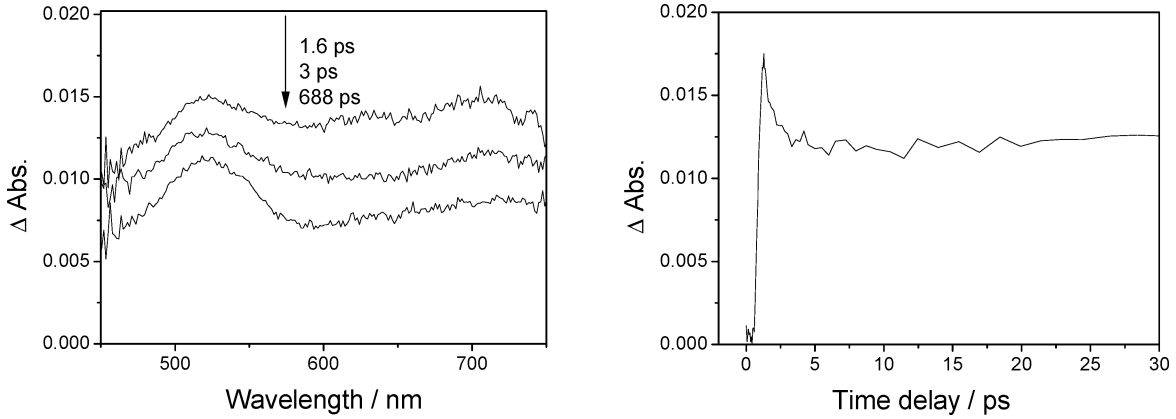

Figure 5. Left: femtosecond transient absorption spectra of benzenethiol nanoparticles in benzene solution, measured after 400 nm excitation. Right: kinetic trace of transient signal measured at 512 nm.

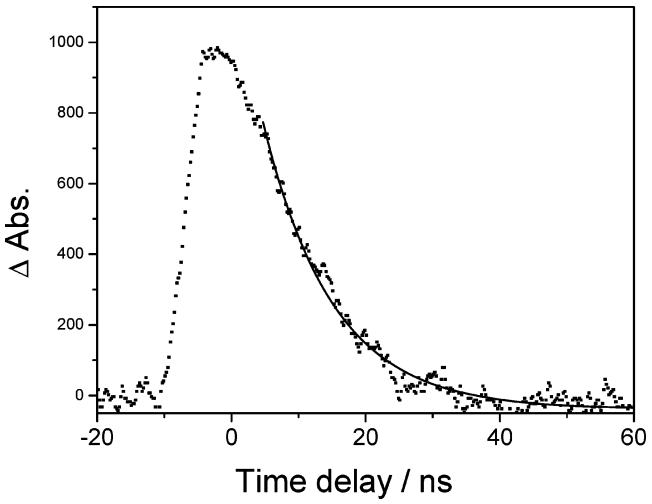

Figure 6. Nanosecond transient absorption decay kinetic trace of benzenethiol nanoparticles in benzene solution, measured after 355 nm excitation and monitored at 580 nm (dotted line, data points; solid line, monoexponential fit). Laser pulse fwhm 6−8 ns.

been synthesized based on the alternative one-phase method[15] and are seen by TEM to be smaller, ranging between 2.1 and 2.3 nm.

It is known that clusters with small sizes and high surface-to-volume ratios undergo substantial scattering between free electrons and the particle surface which, in turn, dampens the surface plasmon.[22] The brown color of the benzenethiol nanoparticles is indicative that the surface plasmon absorption is strongly suppressed and has only a minor contribution to the absorption spectrum (Figure 2). A weak surface plasmon band is possibly present at ca. 550 nm (small inflection in the spectra of Figure 2). The onset of visible absorption at ca. 800 nm and its continuous increase into the UV is characteristic of the interband absorption of bulk gold.[31] The possibility of charge transfer from the gold core to the lowest unocccupied molecular orbitals of the phenyl moiety cannot be ruled out. This possibility seems to be unlikely, however, given the similarity between spectral shape and kinetics of the arenethiol nanoparticles studied herein and previous studies of nanoparticles containing saturated passivating groups.[20,23]

A comparison of the UV/vis absorption spectra of the benzenethiol and its bromo, chloro, and fluoro derivatives shows that all have a very similar shape and relative intensity between 800 and 300 nm. The similarity indicates that the metal particles are of comparable size (2.1−2.3 nm) and do not possess surface plasmon absorptions. It is known from Mie theory that the dielectric properties of the surrounding medium will affect the surface plasmon.[4] Since the interband transition is a bulk property, it is thought to be much less sensitive to the chemical properties of the surrounding medium. In the cases studied herein, the surface plasmon is strongly dampened, with the interband transition contributing primarily to the absorption spectrum. The dominance of the interband transition is evidence of the spectral equivalence within the series of nanoparticles possessing differing passivating groups. To further investigate the physical and chemical properties of the arenethiol monolayer upon the surface plasmon, larger nanoparticles (>5 nm) would be needed.

As expected due to the featureless nature of the interband transition and the weak surface plasmon band (Figure 2), the transient absorption spectra of the benzenethiol nanoparticles are broad. The dip in transient absorption seen at ca. 590 nm could possibly result from a weak plasmon band's bleach superimposed over the broad excited interband absorption. The transient signal shows fast decay that can be fitted to a exponential lifetime of ca. 1 ps; see Figure 5 and Table 2. After the initial decay the same spectral profile is maintained and no further dynamics are observed on the picosecond time scale, with the signal maintaining an amplitude of 60% of its original intensity; see Figure 5. Nanosecond flash photolysis experiments were used to measure the lifetime of the secondary longer lived kinetic component and afforded a lifetime of ca.15 ns (Figure 6). This behavior is quite different from that of nanoparticle systems with intense surface plasmon resonances, which generally show relaxation rates of less than 500 ps.[19,23]

Previously reported 13-atom[32] and 28-atom[20,33] gold clusters also lack surface plasmon absorptions in the visible spectrum. These systems were shown to possess long-lived excited states of molecular nature that correspond to over 60% of the original signal. Furthermore, initial ultrafast ≤1 ps processes were also seen, which reflect relaxation from higher excited states to the lowest, long-lived excited state. The molecular behavior of the 28-atom clusters was also reflected by its independence of the initial decay rates from the laser power.[20] The long-lived transient and the power independence observed here indicate that our benzenethiol nanoparticles behave closer to molecular type clusters than to conventional surface plasmon type nanoparticles.

The halogenated benzenethiol systems all show similar decay profiles, and their lifetimes are summarized in Table 2. The amplitude of decay is also consonant throughout the systems, indicating that the passivating monolayer has little influence on the electronic properties of the gold cluster interband

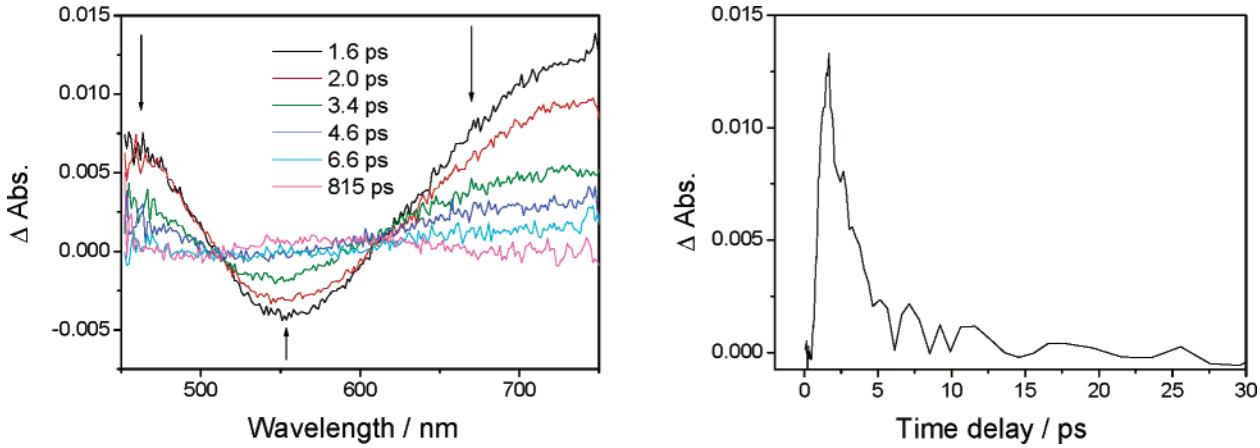

Figure 7. Left: femtosecond transient absorption spectra of biphenylthiol nanoparticles in benzene solution, measured after 400 nm excitation. Right: kinetic trace of transient signal measured at 750 nm.

TABLE 2: Kinetic Fits of Nanoparticle Transient Absorption Spectra, upon 400 nm Excitation in Benzene, and Dielectric Data of Analogous X-Ph Molecules

nanoparticle	Ph-S-NP	Cl-Ph-S-NP	Br-Ph-S-NP	Fl-Ph-S-NP	biphenyl-S-NP	biphenyl-S-NP ($\lambda_{ex.}$ 266 nm, THF)	benzyl-S-NP
λ_{probe}/nm	730	730	730	730	740	750	720
initial decay constant/ps	1.0	0.7	0.7	0.7	2.3	2.7	4.1
amplitude of initial decay constant/%	42	60	52	61	100	100	100
dielectric constant of X-Ph	2.275[a]	5.708[b]	5.4[b]	5.42[c]			

[a] From ref 34. [b] From ref 35. [c] From ref 36.

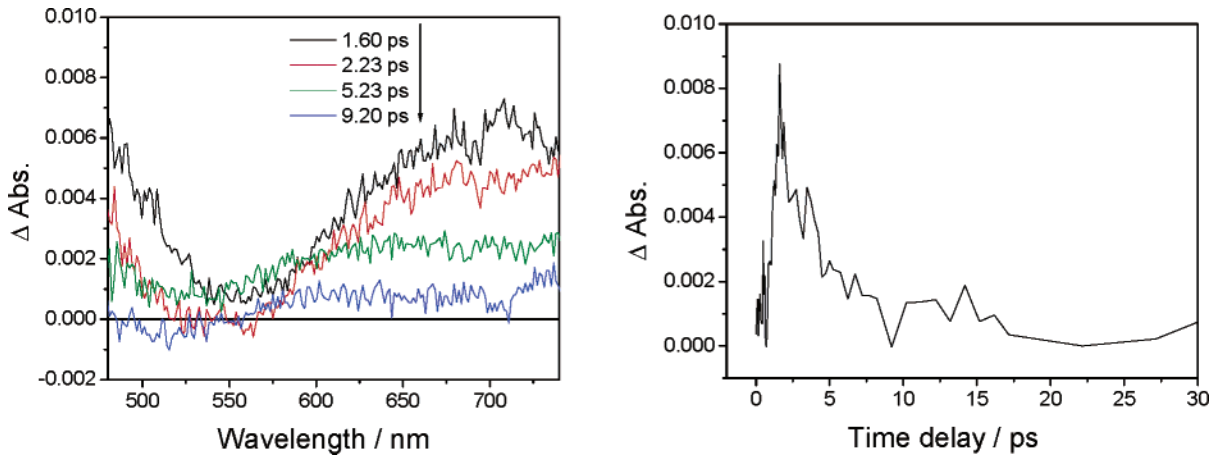

Figure 8. Left: femtosecond transient absorption spectra of benzylthiol nanoparticles in benzene solution, measured after 400 nm excitation. Right: kinetic trace of transient signal measured at 750 nm.

transition. Such an observation is in line with the spectral similarities observed in the absorption spectra and may be rationalized on the same grounds.

Biphenylthiol and Benzylthiol Nanoparticles. The UV/vis spectra of the 3.2 nm biphenylthiol nanoparticles (Figure 2) show a distinct surface plasmon resonance at 555 nm, as expected for nanoparticles of this size.[23] In addition, a biphenyl based $\pi \rightarrow \pi^*$ absorption with maximum at 275 nm is also seen. The UV/vis spectral shape and position of the biphenyl moiety is maintained upon formation of the nanoparticles, an observation pertinent also to the FTIR spectra. The broad absorption covering the visible with an onset at ca. 750 nm results from the interband transitions of the bulk gold. The spectrum of the benzythiol nanoparticles is similar, except for a much broader and less defined surface plasmon absorption.

Femtosecond spectra of the biphenylthiol nanoparticles show a negative transient bleach signal at 555 nm, mirroring its steady-state counterpart, flanked by broad transient absorptions. This behavior is similar to that observed for alkanethiol nanoparticles of similar size.[23] The transient signal results from broadening of the plasmon absorption upon excitation. The decay of the signal has been fitted to a monoexponential function with a lifetime of 2.3 ps. After this process a flat baseline is observed and no more transient signal is present. The observed decay constant is comparable to that seen for alkanethiol nanoparticles[23,25] and can be attributed in all cases to e^-/ph coupling. It was not possible to determine whether the decay is a power-dependent process (as expected for e^-/ph coupling) because the experiments were limited by the induction of decomposition above 0.0072 mJ pulse^{-1}.

No longer secondary decay component is observed for these nanoparticles that could be associated to ph/ph coupling. This can be rationalized by the small size of the particles and hence high surface area to volume ratio, which allow them to undergo efficient heat dissipation to the solvent.[27] The kinetics measured are thought to be the convoluted e^-/ph and ph/ph decay

processes. The presence of the biphenyl moiety in mediating phonon transfer from the nanoparticles into the solvent may also be a contributing factor to the fast relaxation.

Excitation at 266 nm in THF was performed to ascertain whether (i) wavelength effects were seen on the gold clusters decay rates and (ii) excitation of the biphenyl moiety would produce any additional transients originating from the organic based excited state. The fact that the decay lifetime (2.7 ± 0.2 ps) is the same as that obtained in experiments performed at 400 nm excitation indicates that the transient observed is that of the nanoparticle. Free biphenyl-4-thiol-*S*-acetate molecules have singlet excited states with lifetimes into the nanosecond regime. The lack of transient signals from the protecting monolayer on the nanoparticles can be rationalized by its relatively weak intensity in comparison to the excited surface plasmon, and/or by subpicosecond quenching of its excited state by the gold cluster surface plasmon.

Benzylthiol nanoparticles show transient behavior similar to that of the biphenylthiol systems. The surface plasmon bleach can be seen at 550 nm (although, different from the biphenylthiol case, it does not lead to an overall negative signal). A smaller signal-to-noise ratio is evident, and the excited surface plasmon is seen to decay monoexponentially with an approximate lifetime of 4 ps. Similarly to the biphenylthiol case, this rate can be assigned to the e^-/ph coupling of the nanoparticles. Again, the lack of long-lived decay (ph/ph coupling) can be explained by the small size of the nanoparticles[27] and possibly the mediation of benzylthiol based vibrational modes.

Conclusion

This work describes the synthesis and ultrafast photoinduced properties of a series of arenethiol based nanoparticle systems in the small size region, close to the boundary between molecular and surface plasmon type nanoparticle behavior. A variety of nanoparticles have been synthesized with variable sizes and protecting monolayers.

The nanoparticles based on benzenethiol have been synthesized based on a one-phase procedure and form small nanoparticles of between 2.1 and 2.3 nm. Femtosecond transient absorption spectra show dynamics and structure that do not resemble typical spectra for nanoparticles reported in the literature. Spectra exhibit a fast initial decay of ca. 1 ps followed by a long-lived excited state that lives for a few nanoseconds. Theses systems are thought to approach molecular-like behavior, similar to that observed for 28-atom gold clusters. Behavior of the bromo, chloro, and fluoro derivatives is seen to be essentially identical to that of the benzenethiol nanoparticles, indicating that the inequivalence in monolayer properties does not affect the spectral properties of the nanoparticle due to the dampened surface plasmon absorption.

In contrast, biphenyl and benzylthiol protected nanoparticles, which are synthesized using a two-phase procedure, show behavior that is more typical of nanoparticles of dimensions larger than 3−4 nm. The surface plasmon bands are seen to be present with maxima around 550 nm. Femtosecond results show fast decays of 2.32 and 4.06 ps for the biphenyl and benzylthiol systems, respectively.

This study is the first report into the ultrafast optical properties of arenethiol based nanoparticles. It has provided insight into the synthetic and spectral features of these nanoparticles. The chemical ease of further functionalizing the aromatic passivating layer is currently being exploited to synthesize novel arenethiol based chromophore passivated nanoparticles. These nanoparticles will be studied with the intention of further understanding the interaction between molecular excited states and the nanoparticles.

Acknowledgment. The authors thank M. A. Rampi for useful discussions and S. Carli for the synthesis of biphenyl-4-thiol-*S*-acetate. Funding by the EC (Grant G5RD-CT-2002-00776, MWFM) and MIUR (Grant FIRB-RBNE019H9K) is gratefully acknowledged.

Supporting Information Available: NMR spectra of nanoparticle systems. Size distribution histograms of nanoparticle systems. This material is available free of charge via the Internet at http://pubs.acs.org.

References and Notes

(1) Brust, M.; Walker, M.; Bethell, D.; Schriffrin, D. J.; Whyman, R. *J. Chem. Soc., Chem. Commun.* **1994**, 801.
(2) Templeton, A. C.; Wuelfing, W. P.; Murray, R. W. *Acc. Chem. Res.* **2000**, *33*, 27.
(3) Daniel, M.; Astruc, D. **2004**, *104*, 293.
(4) Templeton, A. C.; Pietron, J. J.; Murray, R. W.; Mulvaney, P. *J. Phys. Chem. B* **2000**, *104*, 564.
(5) Thomas, K. G.; Kamat, P. V. *Acc. Chem. Res.* **2003**, *36*, 888.
(6) Imahori, H.; Fukuzumi, S. *Adv. Mater.* **2001**, *13*, 1197.
(7) Daniel, M.; Astruc, D. *Chem. Rev.* **2004**, *104*, 293.
(8) Lahav, M.; Heleg-Shabtai, V.; Wasserman, J.; Katz, E.; Willner, I.; Dürr, H.; Hu, Y.-Z.; Bossmann, S. H. *J. Am. Chem. Soc.* **2000**, *122*, 11480.
(9) Fox, M. A. *Acc. Chem. Res.* **1999**, *32*, 201.
(10) Alvarez, M. M.; Khoury, J. T.; Schaaff, T. G.; Shafigullin, M. N.; Vezmar, I.; Whetten, R. L. *J. Phys. Chem. B* **1997**, *101*, 3706.
(11) Templeton, A. C.; Hostetler, M. J.; Warmouth, E. K.; Chen, S.; Hartshorn, C. M.; Krishnamurthy, V. M.; Forbes, M. D. E.; Murray, R. W. *J. Am. Chem. Soc.* **1998**, *120*, 4845.
(12) Price, R. C.; Whetten, R. L. *J. Am. Chem. Soc.* **2005**, *127*, 13750 and references therein.
(13) Brust, M.; Fink, J.; Bethell, D.; Schriffrin, D. J.; Kiely, C. *J. Chem. Soc., Chem. Commun.* **1995**, 1655.
(14) Chen, S.; Murray, R. W. *Langmuir* **1999**, *15*, 682.
(15) Grate, J. W.; Nelson, D. A.; Skaggs, R. *Anal. Chem.* **2003**, *75*, 1868.
(16) Evans, S. D.; Johnson, S. R.; Cheng, Y. L.; Shen, T. *J. Mater. Chem.* **2000**, *10*, 183.
(17) Montalti, M.; Prodi, L.; Zacceroni, N.; Beltrame, M.; Morotti, T.; Quici, S. Submitted for publication.
(18) Joo, S. *Chem. Lett.* **2004**, *33*, 60.
(19) Link, S.; El-Sayad, M. A. *J. Phys. Chem. B* **1999**, *103*, 8410.
(20) Link, S.; El-Sayed, M. A.; Schaaff, T. G.; Whetten, R. L. *Chem. Phys. Lett.* **2002**, *356*, 240.
(21) Schaaff, T. G.; Shafigullin, M. N.; Khoury, J. T.; Vezmar, I.; Whetten, R. L.; Cullen, W. G.; First, P. N.; Gutiérrez-Wing, C.; Ascensio, J.; Jose-Yacamán, M. J. *J. Phys. Chem. B* **1997**, *101*, 7885.
(22) Hodak, J. K.; Henglein, A.; Hartland, G. V. *J. Chem. Phys.* **2000**, *112*, 5942.
(23) Logunov, S. L.; Ahmadi, T. S.; El-Sayed, M. A.; Khoury, J. T.; Whetten, R. L. *J. Phys. Chem. B* **1997**, *101*, 3713.
(24) Hohlfeld, J.; Wellershoff, S. S.; Güdde, J.; Conrad, U.; Jähnke, V.; Matthias, E. *Chem. Phys.* **2000**, *251*, 237.
(25) Shin, H. J.; Hwang, I.; Hwang, Y.; Kim, D.; Han, S. H.; Lee, J.; Cho, G. *J. Phys. Chem. B* **2003**, *107*, 4699.
(26) Hodak, J. K.; Henglein, A.; Hartland, G. V. *J. Phys. Chem. B* **2000**, *104*, 9954.
(27) Hu, M.; Hartland, G. V. *J. Phys. Chem. B* **2002**, *106*, 7029.
(28) Chiorboli, C.; Rogers, M. A. J.; Scandola, F. *J. Am. Chem. Soc.* **2003**, *125*, 483.
(29) Prodi, A.; Indelli, M. T.; Kleverlaan, C. J.; Scandola, F.; Alessio, E.; Gianferrara, T.; Marzilli, L. G. *Chem.*—Eur. J. **1999**, *5*, 2668.
(30) Donkers, R. L.; Song, Y.; Murray, R. W. *Langmuir* **2004**, *20*, 4703.
(31) Henglein, A. *Langmuir* **1999**, *15*, 6738.
(32) Smith, B. A.; Zhang, J. Z.; Giebel, U.; Schmid, G. *Chem. Phys. Lett.* **1997**, *270*, 139.
(33) Link, S.; Beeby, A.; FitzGerald, S.; El-Sayad, M. A.; Schaaff, T. G.; Whetten, R. L. *J. Phys. Chem. B* **2002**, *106*, 3410.
(34) Murov, S. L. *Handbook of Photochemistry*; Dekker: New York, 1973.
(35) *CRC Handbook of Chemistry and Physics*; Lide, D. R., Ed.; CRC Press: Boca Raton, FL, 2004; Vol. 85.
(36) Baumann, W.; Nagy, Z. *Pure Appl. Chem.* **1993**, *65*, 1729.